Order−Disorder Transition in Comblike Block Copolymers Obtained by Hydrogen Bonding between Homopolymers and End-Functionalized Oligomers: Poly(4-vinylpyridine)−Pentadecylphenol

Janne Ruokolainen,[†] Mika Torkkeli,[‡] Ritva Serimaa,[‡] Erny Komanschek,[§] Gerrit ten Brinke,*[,†,▽] and Olli Ikkala*[,†]

Department of Engineering Physics and Mathematics, Helsinki University of Technology, Rakentajanaukio 2, FIN-02150 Espoo, Finland, Department of Physics, University of Helsinki, P.O. Box 9, FIN-00014 Helsinki, Finland, SERC Daresbury Laboratory, Warrington WA4 4AD, United Kingdom, and Department of Polymer Science and Materials Science Center, University of Groningen, Nijenborgh 4, 9747 AG Groningen, The Netherlands

Received October 30, 1996; Revised Manuscript Received January 22, 1997[⊗]

ABSTRACT: Dynamic mechanical spectroscopy (DMS) is used to further investigate the recently observed order−disorder transition (ODT) in comblike block copolymers obtained by hydrogen bonding between poly(4-vinylpyridine) and pentadecylphenol (P4VP−PDP$_x$). For stoichiometric amounts of pyridine and phenol, i.e., $x = 1.0$, the ODT to a lamellar structure occurs at $T \simeq 65$ °C. The dynamic moduli G' and G'' simultaneously show a crossover from a liquidlike behavior ($G' \sim \omega^{1.5}$ and $G'' \sim \omega$) to a response intermediate between a Newtonian fluid and a solid ($G' \approx G'' \sim \omega^{1/2}$). The behavior above T_{ODT} differs slightly from a homopolymer melt ($G' \sim \omega^{2.0}$) due to composition fluctuations, whereas the behavior below T_{ODT} is characteristic for quenched block copolymer lamellar phases with local uniaxial order and global isotropy. Near room temperature, a transition to solid behavior ($G \sim \omega^0$) takes place due to crystallization of the alkyl side chains. Larger amounts of PDP lower the T_{ODT} temperature, and for $x = 2.0$ the transition to solid response occurs directly from the disordered state. Small and wide angle X-ray scattering (SAXS and WAXS) experiments and differential scanning calorimetry (DSC) corroborate these findings. Furthermore, SAXS and WAXS demonstrate that the low-temperature state of P4VP−PDP$_{2.0}$ is not stable and indicate that ultimately macrophase separation into a pure crystalline PDP phase and a microphase separated P4VP−PDP phase occurs.

Introduction

Block copolymer systems have been studied extensively during the last decades and continue to attract the interest of experimentalists and theoreticians alike. Composed of at least two different polymer blocks, immiscibility of these blocks induces self-assembly into various ordered microstructures. Until now at least six different microphases have been discovered in diblock copolymer melts. These include the three traditional structures, periodically arranged spheres, hexagonally packed cylinders, and lamellar, and the three new phases which have been discovered only very recently: hexagonally modulated lamellar, hexagonally perforated layers, and bicontinuous "gyroid".[1] Block copolymer melts usually (i.e., the UCST situation) form disordered phases at elevated temperatures where the different blocks are homogeneously mixed. The order−disorder temperature T_{ODT} of block copolymers is defined as the temperature at which the ordered microdomain structures disappear completely during heating or begin to appear during cooling. A theoretical review of block copolymers can be found in a very recent article by Matsen and Bates[2] and in the classical review by Fredrickson and Bates.[3]

The rheological properties of block copolymers near the order−disorder temperature T_{ODT} are quite different from homopolymer melts. A most recent review by Fredrickson and Bates[1] deals extensively with various aspects of block copolymer rheology. Dynamic mechanical spectroscopy (DMS) has turned out to be a very efficient tool to determine the position of the T_{ODT}, to study the order−disorder transition behavior,[4−17] and even in some cases to discriminate between different morphologies.[18] There are several methods to determine T_{ODT} from rheological data. In some cases the T_{ODT} can be determined from viscosity measurements as a function of temperature, where it corresponds to the temperature where the Newtonian type viscosity is observed for the first time during heating.[4−7] Another method is to use isothermal frequency scans at various temperatures. At the T_{ODT} the dynamic storage modulus $G'(\omega)$ or the dynamic loss modulus $G''(\omega)$ shows an abrupt drop as a function of temperature.[7−14] Han and co-workers[13−17] proposed the use of log−log plots of $G'(\omega)$ versus $G''(\omega)$. The T_{ODT} then would correspond to the temperature where log G' versus log G'' plots become independent of temperature during heating from the microphase-separated state.

In this article we will consider a completely different class of copolymer systems obtained by hydrogen bonding between homopolymers and end-functionalized oligomers. In this way highly polydisperse mixtures of comblike copolymer structures, based on reversible rather than covalent bonding, are obtained.[19] We will focus on a particular system, poly(4-vinylpyridine)−pentadecylphenol (P4VP−PDP$_x$, where x represents the ratio between the number of phenol and pyridine groups). It has recently been demonstrated that this kind of system exhibits an order−disorder transition (ODT); for $x = 1$, it occurs at $T \cong 65$ °C.[20,21] Many similarities exist with conventional comb copolymer

[†] Helsinki University of Technology.
[‡] University of Helsinki.
[§] SERC Daresbury Laboratory.
[▽] University of Groningen.
[⊗] Abstract published in *Advance ACS Abstracts,* March 1, 1997.

S0024-9297(96)01609-9 CCC: $14.00

systems, which have been discussed in some detail in the literature.[22−25] However, due to the reversible nature of the side chain attachment, there are also interesting differences which potentially may lead to very rich phase behavior.[26,27] It is well established that by using suitable end-functionalized oligomers, self-organized mesomorphic structures may be obtained from flexible polymers, usually of a lamellar type.[20,21,28−33] In the case of polyelectrolytes complexed with surfactants, evidence for a hexagonal structure and some other morphologies, such as egg-carton, has been presented as well.[34−36] For the stoichiometric polyelectrolyte−surfactant systems, the microphase-separated morphologies are very stable, and phase transitions are not observed nor is the possibility discussed. The strong ionic interaction and the large polar−nonpolar repulsion favor mesomorphic structures and prevent the occurrence of an ODT under normal conditions. However, and this is one of the biggest advantages of using weaker interactions, order−disorder transitions are present in suitable polymer systems involving end-functionalized oligomers which interact with the polymer via hydrogen bonding.[20,21,33]

Comblike copolymer systems based on association between homopolymers and end-functionalized oligomers have definite advantages compared to conventional comb copolymer systems. They are very easy to "synthesize" and offer a simple method to vary the number and the length of the "combs" by simply varying the oligomer mole fraction x and the length of the oligomers. The possibility to change the strength of the polymer−oligomer interaction gives yet another parameter to tailor the behavior. The interaction strength of the association can be varied from an almost permanent ionic bonding[28,30] to weak secondary interactions.[20,33,37] In many cases these systems are also very ideal to study experimentally. They are often much better organized than many block copolymer systems, and due to a very intensive small angle X-ray scattering (SAXS) pattern, they allow the use of relatively short measuring times in a conventional SAXS setup; therefore, high temperature resolution measurements over an extended temperature interval are feasible.

In this paper we will report for the first time the rheological behavior of a particular representative of this class of comblike copolymer systems, i.e., P4VP−PDP$_x$. We use both rheological measurements and X-ray scattering data to address the behavior of the system near the order−disorder transition and will discuss briefly the interference of the crystallization of the side chains with the ODT for more than stoichiometric amounts of PDP.

Experimental Section

Materials and Sample Preparation. The atactic P4VP was acquired from Polyscience Europe GmbH. The viscosity average molecular weight M_v = 49 000 g/mol. 3-Pentadecylphenol (PDP) was purchased from Bauer & Pfaltz (purity 97%). Chloroform was of analysis grade and was carefully dried by 3 Å molecular sieves. P4VP and PDP were first dried at 60 °C in vacuum for 2 days. P4VP−PDP$_x$ complexes were prepared from chloroform solutions. Here x denotes the number of phenol groups per vinylpyridine repeat unit. We will consider mostly the nominally fully complexed case, i.e., x = 1.0. The PDP and the solvent were first mixed together until a clear solution was obtained. P4VP was subsequently added followed by mechanical stirring for approximately 1 h at room temperature. The concentrations of polymer in the solvent were kept low (less than 1 wt %) to ensure homogenous complex formation. Chloroform was evaporated on a hot plate at 50 °C. The complexes were further dried at 60 °C in vacuum for at least 2 days and subsequently stored in a desiccator.

Rheological Measurements. The dynamic storage and loss moduli, $G'(\omega)$ and $G''(\omega)$, were measured using a Bohlin VOR rheometer in oscillation mode in the frequency range $0.01 \leq \omega/2\pi$ (Hz) ≤ 20 at temperatures between 20 and 90 °C. Measurements were performed during slow cooling (approximately 0.2−0.3 °C/min). The measuring geometry was concentric cylinder C 14, which consists of a fixed bob (inner cylinder, diameter 14 mm and cone angle 15°) located in a rotating cup (outer cylinder, diameter 15.4 mm). Below the ODT, small strain amplitudes of 1−2% were used (0.001−0.01 strain), and above the ODT at high temperatures and low frequencies, strain amplitudes up to 30% were used (strain less than 0.1), which are all well within the linear viscoelastic range.

Small Angle X-ray Scattering. A sealed fine focus Cu X-ray tube was used in a point-focusing mode. The Cu Kα (λ = 1.542 Å) radiation is monochromatized with a Ni filter and a totally reflecting glass block (Huber small angle chamber 701). The scattered radiation is detected in the horizontal (beam width) direction by a linear one-dimensional proportional counter (MBraun OED-50M). The space between sample and detector is evacuated to 0.05 mmHg using 13 μm polyimide foils as X-ray windows. The beam height is limited by two horizontal slits with approximately 1 mm aperture, one before the sample and another in front of the detector. Also, a narrow vertical slit is placed before the sample to reduce background scattering. The fwhm of the beam width is below 0.002 Å^{-1}, and the instrumental function in the vertical direction, due to beam height and detector height profiles, is determined to have fwhm = 0.048 Å^{-1}. Owing to this, no correction for the experimental smearing is necessary in the current analysis. The small angle scattering was recorded at various temperatures.

Additional measurements were performed at beamline 8.2 of the Synchrotron Radiation Source in Daresbury, U.K., using a beam of λ = 1.52 Å X-rays measuring 3 × 0.3 mm^2 at the sample position. The SAXS data were collected with a Daresbury quadrant detector, the wide angle X-ray scattering (WAXS) data were acquired with a curved INEL detector, and a DSC unit, which is a modified Linkham THM microscope hot stage, was used for thermal data collection. More details about the setup can be found in a recent publication by Bras et al.[38]

Results

Mesomorphic structures in comblike copolymers obtained by hydrogen-bonding association between flexible polymers and end-functionalized oligomers have been discussed in length in our previous papers.[20,21,37,39] The presence of an order−disorder transition in P4VP−PDP$_x$ was first reported in ref 21, and here we will address this system in more detail, emphasizing dynamic mechanical spectroscopy. So far, we have not been able to obtain good transmission electron microscopy data, and our knowledge about the mesomorphic structures rests solely on the SAXS data. The presence of a faint second-order peak at 2 times the first-order peak wave vector indicates that this particular system for various compositions x organizes in the form of lamellae. Figure 1 presents a picture of the hydrogen-bonding interaction between P4VP and PDP as well as an oversimplified picture of the lamellar morphology. Bates and coworkers[1,18] demonstrated that DMS can also offer a kind of fingerprint of the microphase-separated morphology, at least for diblock copolymers. In pure diblocks and binary blends of polyethylene-poly(ethylethylene), five different structures were identified: spherical (S), cylindrical (C), gyroid (G), hexagonally perforated layers (HPL), and lamellar (L). In particular the S, G, and HPL phases displayed a considerably different DMS behavior from that of the L and C structures.

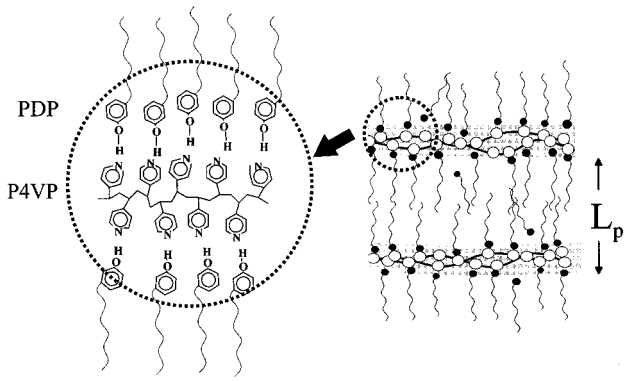

Figure 1. Schematic illustrations of P4VP−PDP hydrogen bonding and lamellar microphase-separated structure.

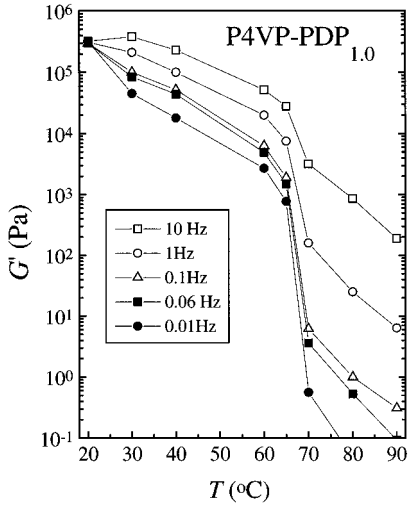

Figure 2. Temperature dependence of the dynamic storage modulus G' of P4VP−$PDP_{1.0}$ at various frequencies ω.

Rheology. At the order−disorder transition, the low-frequency dynamic storage modulus G' is known to show a precipitous drop upon heating from the ordered phase. In fact, the measurement of G' at a fixed frequency during slow heating is one of the most convenient methods to determine the T_{ODT}. Figure 2 shows the isochronal dynamic shear storage modulus of P4VP−$PDP_{1.0}$ as a function of temperature. Especially at low frequencies a steep drop occurs at approximately 65 °C, which corresponds to the transition temperature as determined from the SAXS data, which will be presented further on. Log−log plots of G' and G'' versus ω of the same system are presented in Figure 3. As before, at temperatures between 65 and 70 °C an abrupt drop in the dynamic storage and loss moduli occurs at low frequencies. At temperatures below 65 °C we find $G'(\omega) \approx G''(\omega) \sim \omega^{0.5}$, which is the typical behavior reported for lamellar morphologies of ordinary di- and triblock copolymers and which supports the model presented in Figure 1. At temperatures of 70 °C and higher we find $G'(\omega) \sim \omega^{1.5}$ and $G''(\omega) \sim \omega^{1.0}$. Values of 2.0 and 1.0, respectively, are predicted and found for these exponents in simple homopolymer melts.[40,41] The fact that for temperatures above the T_{ODT} the frequency dependence of G' deviates slightly from the terminal zone limit behavior is generally attributed to pretransitional composition fluctuations which may persist as far as 50 °C above the transition temperature.[8,12,42,43] At low temperatures G' and G'' become independent of the oscillation frequency ω which can be attributed to the alkyl side chain crystallization.

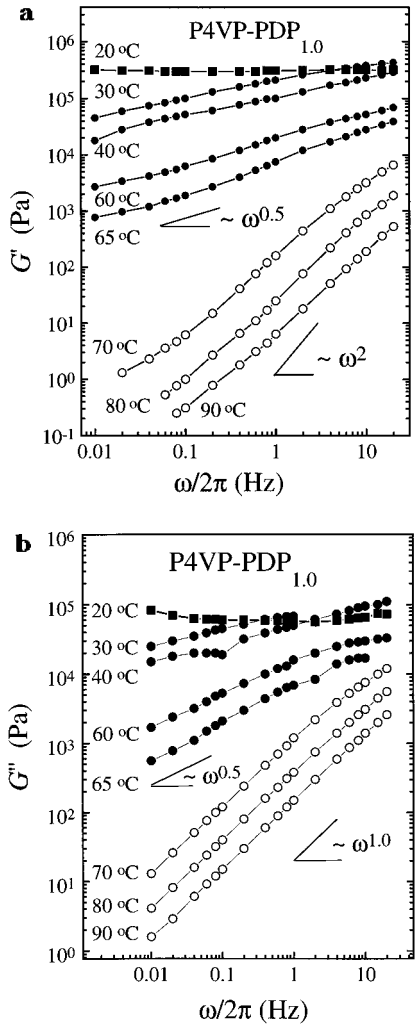

Figure 3. Isothermal frequency scans of the (a) dynamic storage modulus G' of P4VP−$PDP_{1.0}$ at various temperatures and (b) the dynamic loss modulus G'' of P4VP−$PDP_{1.0}$ at various temperatures.

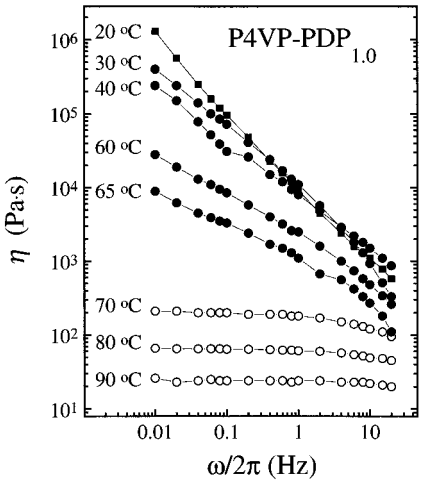

Figure 4. Dynamic viscosity $\eta \equiv G''(\omega)/\omega$ for P4VP−$PDP_{1.0}$ as a function of frequency for various temperatures.

Similar conclusions follow from the behavior of the dynamic viscosity η, defined by $\eta \equiv G''(\omega)/\omega$, shown in Figure 4. At temperatures above the order−disorder temperature the viscosity is frequency-independent (Newtonian), but when the temperature is lowered below T_{ODT} the viscosity exhibits strong nonlinear yield (non-Newtonian). This behavior is yet another mani-

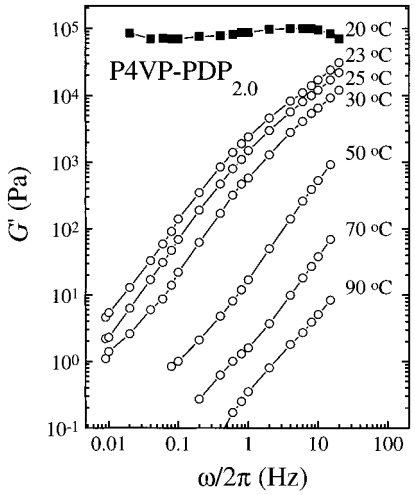

Figure 5. Isothermal frequency scans of the dynamic storage modulus G' of P4VP−$PDP_{2.0}$ at various temperatures.

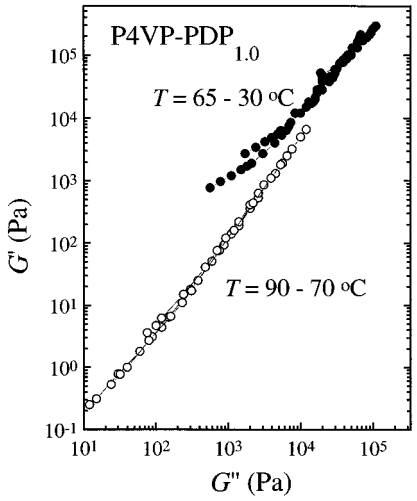

Figure 6. Plot of log G' versus log G'' for P4VP−$PDP_{1.0}$ at various temperatures.

festation of a phase transition from a disordered to an ordered state.[8]

We also measured the dynamic storage moduli G' for a P4VP−$PDP_{2.0}$ sample which contains twice as many phenol groups as pyridine groups. In P4VP−PDP systems an excess amount of PDP leads to a reduction of the ODT temperature,[21] which is remarkable in the light of very recent calculations by Tanaka and co-workers,[27] predicting the exact opposite behavior. In the case of $x = 1.5$, the order−disorder transition coincides with the crystallization of the alkyl side chains.[21] For still higher values and hence also for $x = 2.0$, the T_{ODT} is below the crystallization temperature of the alkyl chains and the crystallization intervenes before the ODT is reached. This can be seen clearly in Figure 5 which presents a log−log plot of G' versus ω. At high temperatures it exhibits the typical behavior of homopolymer melts with a slope of approximately 1.5, and during slow cooling the material remains liquidlike until the sample crystallizes at 20 °C and $G'(\omega) \sim \omega^0$.

Han and co-workers[13,14,16,44] suggested that log−log plots of G' versus G'' become virtually independent of temperature at T_{ODT} and that this can be used as another criterion to determine the transition temperature. Above the ODT the slope of this curve should be equal to 2.0, which is the typical value for homopolymer or random copolymer melts in the terminal zone. However, Adams et al.[45] showed that in some cases the G' versus G'' curves show a temperature dependence well beyond the order−disorder transition temperature and thus leads to a substantial overestimation of T_{ODT}. As noted before, Bates and co-workers[9,12] attribute this temperature dependence of the G' versus G'' above the T_{ODT} to the presence of composition fluctuations. Figure 6 presents a log−log plot of G' versus G'' for our P4VP−$PDP_{1.0}$ system. Above the ODT the behavior is independent of the temperature with a slope of approximately 1.5, but the behavior is also independent of temperature below the ODT, only with a slightly smaller slope. Therefore, in our case we can only determine the T_{ODT} from these kinds of plots from the point where the slope of the curve shows an abrupt change, but there is, of course, no reason to use these kinds of plots for this purpose since much better alternatives are available.

Small Angle X-ray Scattering. It is possible to determine the ODT temperature very accurately by small angle X-ray scattering using scattering experiments with high temperature resolution. Experiments with a low temperature resolution (temperature increment > 10 °C) may overlook the sharpness of the ODT and lead to an inaccurate determination of the T_{ODT}.[46] Our in-house SAXS device allows measurements with a small temperature increment (<0.2 °C) and a very high accuracy. This enables us to determine the order−disorder transition temperature with an accuracy better than ±0.5 °C. Figure 7 shows the thus obtained SAXS patterns for P4VP−$PDP_{1.0}$ as a function of temperature during slow cooling (0.02 °C /min) from 70 to 50 °C. Each frame corresponds to a 0.25 °C temperature interval. The most striking feature in the figure is the strong increase of scattering upon approaching 65 °C, and at ca. 63 °C the scattering intensity is saturated. An exothermic DSC peak and the appearance of birefringence in optical microscopy measurements are observed simultaneously with the appearance of this sharp almost singular small angle scattering peak,[47] confirming the order−disorder nature of the transition. The measurements were also performed during slow heating, and the results were identical with those obtained during cooling, not showing any hysteresis behavior. The structure is proposed to be a lamellar morphology as judged from the SAXS patterns. The first-order diffraction peak is very sharp, and although not visible in Figure 7, a very weak second-order diffraction peak exists at a scattering vector of 2 times the value of the first-order scattering maximum.[21]

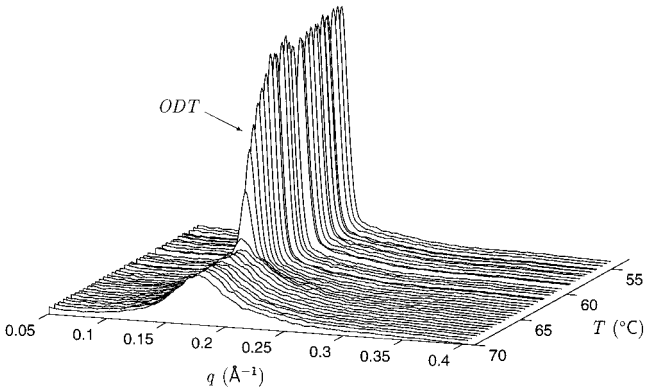

Figure 7. SAXS profiles of P4VP−$PDP_{1.0}$ measured at 0.25 °C intervals during cooling with 0.02 °C/min.

There are various ways to determine accurately the ODT temperature from SAXS measurements: (i) a plot

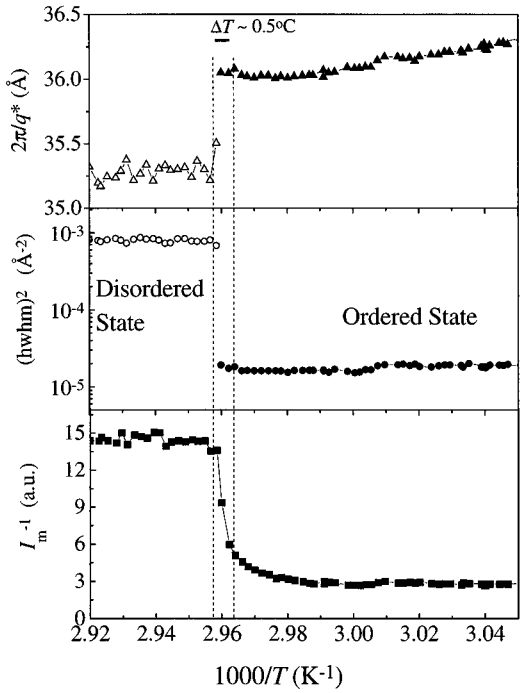

Figure 8. (Bottom) Reciprocal of the maximum of the scattering intensity $1/I_{max}$ as a function of $1000/T$ (K^{-1}). (Middle) Square of half-width of half-maximum [$(hwhm)^2$] as a function of $1000/T$ (K^{-1}). (Top) Characteristic wavelength of the dominant fluctuation $2\pi/q^*$ as a function of $1000/T$ (K^{-1}).

of the reciprocal of the intensity of the diffraction peak ($1/I_{max}$) versus reciprocal absolute temperature ($1/T$) and (ii) a plot of the wavelength of the dominant mode D of the concentration fluctuation (below the T_{ODT} D is the long period of the lamellar structure) versus $1/T$. The value of D is obtained from the relation $D = 2\pi/q^*$, where q^* is the characteristic scattering vector of the peak position of the SAXS pattern. Recently T_{ODT} has been determined as well by employing plots of the square of the half-width of the half-maximum [$(hwhm)^2$] versus $1/T$. This method was first introduced by Stühn et al.[48] and Ehlich et al.[49] These plots will show a sudden change or in some cases a nearly discontinuous drop when exceeding the ODT.

Here we have applied these methods for our P4VP−$PDP_{1.0}$ system, and Figure 8 presents the plots of $1/I_{max}$, $(hwhm)^2$, and $1/D$ versus $1/T$. All curves show a precipitous or discontinuous drop near the ODT. The plot of $1/I_{max}$ versus $1/T$ was obtained with a temperature decrement of 0.25 °C during very slow cooling (0.02 °C/min) and shows a very sharp change between 64.5 and 65.0 °C. From this curve it follows that $T_{ODT} = 64.8 \pm 0.3$ °C. Above that temperature $1/I_{max}$ decreases linearly as a function of $1/T$. In the ordered lamellar state the intensity is almost independent of temperature. The sharpness of the first-order scattering maximum shows also a very clear transition near the ODT temperature. At the order−disorder transition, the square of the hwhm decreases nearly 2 orders of magnitude as can be seen from the middle part of Figure 8 (notice the logarithmic y-scale). The peak sharpness is almost constant below and above the T_{ODT}. The uppermost part of Figure 8 depicts $2\pi/q^*$ versus $1/T$. At high temperatures there exists only a broad scattering maximum due to the characteristic comb−polymer-like composition fluctuations, and the peak position remains almost constant as a function of temperature. As T_{ODT} is approached, a sharp peak starts to develop at a smaller angle which corresponds to 36.1 Å, approximately 1.0 Å larger than that of $2\pi/q^*$ in the homogeneous state. Below the T_{ODT} the peak shifts to smaller angles almost linearly with $1/T$ and reaches 38.0 Å at a temperature of 25 °C. The value of the T_{ODT} obtained from the SAXS measurements is within experimental error equal to the one determined from the rheological measurements.

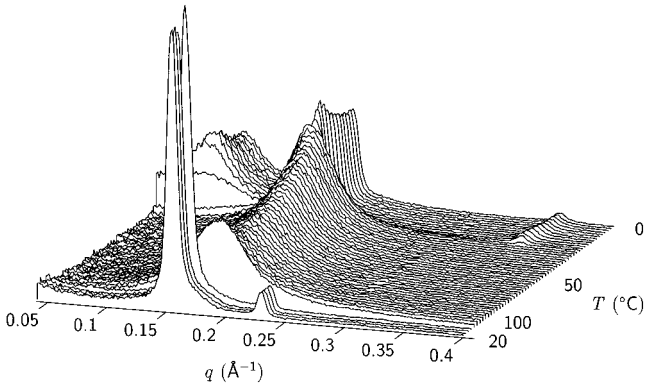

Figure 9. SAXS profiles of P4VP−$PDP_{2.0}$ as a function of temperature. After fast heating from room temperature to 100 °C, the sample was slowly cooled with 5 °C/min to 0 °C.

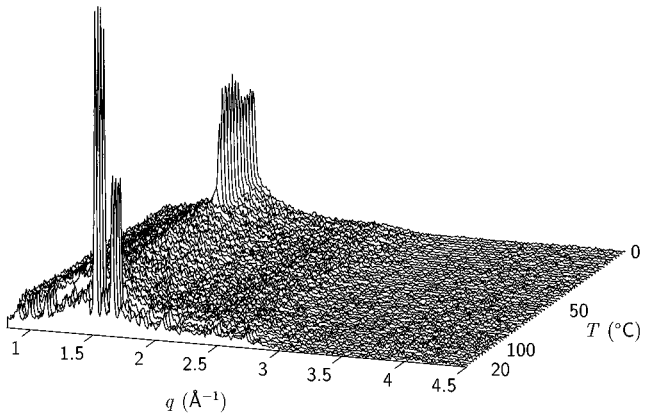

Figure 10. WAXS profiles of P4VP−$PDP_{2.0}$ obtained simultaneously with the SAXS profiles presented in Figure 9.

Finally, Figure 9 shows the results of SAXS measurements on the system P4VP−$PDP_{2.0}$, as performed at Daresbury Laboratory. The first frame corresponds to room temperature, and subsequent frames were obtained during fast heating to 100 °C followed by slow cooling with 5 °C/min to 0 °C. The SAXS pattern of the original sample (first frame), which had been kept in an uncontrolled manner near room temperature for some days, shows two prominent diffraction peaks. The second peak (largest scattering vector) is characteristic for crystalline pure PDP, which we know to be present in the sample from the WAXS data presented in Figure 10. This observation follows from the fact that crystalline pure PDP exhibits a 110 and 200 reflection,[20] just as in the first few frames in Figure 10, whereas crystalline PDP associated with P4VP shows only a single 110 reflection. This confirms our previous observations that for a large excess of PDP, macrophase separation will ultimately take place. The whole issue of macrophase separation is of considerable interest, since recent theoretical work claims that macro *fluid*−*fluid* phase separation should occur in this kind of system for a large excess of either component.[27] Our observations do not really confirm this statement, since the macrophase separation may well be due to the crystallization. The sharp first peak in the SAXS

pattern (first few frames) corresponds to the microphase structure of the remaining P4VP−PDP phase. After melting, a correlation hole peak is present from 100 to 20 °C, where the peak sharpens and at the same time a very clear second-order peak appears. Simultaneously taken DSC and WAXS measurements (Figure 10) show that this transition corresponds to the crystallization of the alkyl side chains (i.e., only one peak), in full agreement with the DMS data presented before. The SAXS pattern at low temperatures is, however, completely different from the original SAXS pattern (first few frames) and resembles the SAXS patterns of crystallized samples of P4VP−PDP_x for values of $x \leq 1.5$. At this stage we are apparently still dealing with a microphase-separated structure. Nevertheless, the presence of considerable scattering at the smallest angles shows the presence of density fluctuations on a much larger scale. To a lesser extent this has been observed before for smaller values of x.[21]

Concluding Remarks

In this paper we have demonstrated that dynamic mechanical spectroscopy remains a powerful tool to investigate the nature and the temperature of order−disorder transitions in comblike copolymer systems obtained by polymer−oligomer association. The linear dynamic mechanical properties of our systems do not differ in an essential way from the well-established properties of di- and triblock copolymers, at least not in the most simple case of lamellar structures. So far, we have not found structures other than lamellae, but we hope to address this issue by using longer alkylphenol oligomers in the near future.

Although the microphase separation in P4VP−PDP_x has now been discussed in some detail, the T,x phase diagram is still far from complete. The theoretical work of Tanaka and co-workers[27] shows that it is of particular interest to investigate more carefully the $x \gg 1$ case. In more general terms, theoretically one of the most challenging problems concerns the nature of the microphase-separated structures of these polydisperse thermoreversible comblike polymer systems. This is a function of composition (=x), length of the end-functionalized oligomers, and strength of the interactions, both attractive and repulsive. Work along this line is in progress now.

Acknowledgment. We acknowledge Heikki Tenhu of Helsinki University for permission to use the dynamic rheometer. This work has been supported by Finnish Academy, Technology Development Centre (Finland), and Neste Foundation.

References and Notes

(1) Fredrickson, G. H.; Bates, F. S. *Annu. Rev. Mater. Sci.* **1996**, *26*, 501.
(2) Matsen, M. W.; Bates, F. S. *Macromolecules* **1996**, *29*, 1091.
(3) Bates, F. S.; Fredrickson, G. H. *Annu. Rev. Phys. Chem.* **1990**, *41*, 525.
(4) Chung, C. I.; Gale, J. C. *J. Polym. Sci., Polym. Phys. Ed.* **1976**, *14*, 1149.
(5) Chung, C. I.; Lin, M. T. *J. Polym. Sci., Polym. Phys. Ed.* **1978**, *16*, 545.
(6) Wildmaier, J. M.; Meyer, G. C. *J. Polym. Sci., Polym. Phys. Ed.* **1980**, *18*, 2217.
(7) Gouinlock, E. V.; Porter, R. S. *Polym. Eng. Sci.* **1977**, *17*, 535.
(8) Bates, F. S. *Macromolecules* **1984**, *17*, 2607.
(9) Rosedale, J. H.; Bates, F. S. *Macromolecules* **1990**, *23*, 2329.
(10) Gehlsen, M. D.; Almdal, K.; Bates, F. S. *Macromolecules* **1992**, *25*, 939.
(11) Almdal, K.; Bates, F. S.; Mortensen, K. *J. Chem. Phys.* **1992**, *96*, 9122.
(12) Bates, F. S.; Rosedale, J. H.; Fredrickson, G. H. *J. Chem. Phys.* **1990**, *92*, 6255.
(13) Han, C. D.; Baek, D. M.; Kim, J. K.; Ogawa, T.; Sakamoto, T.; Hashimoto, T. *Macromolecules* **1995**, *28*, 5043.
(14) Han, C. D.; Baek, D. M.; Kim, J. K. *Macromolecules* **1990**, *23*, 561.
(15) Han, C. D.; Kim, J. *J. Polym. Sci., Polym. Phys. Ed.* **1987**, *25*, 1741.
(16) Han, C. D.; Kim, J.; Kim, J. K. *Macromolecules* **1989**, *22*, 383.
(17) Han, C. D.; Baek, D. M.; Sakurai, S.; Hashimoto, T. *Polym. J.* **1989**, *21*, 841.
(18) Zhao, J.; Majumdar, B.; Schulz, M. F.; Bates, F. S.; Almdal, K.; Mortensen, K.; Hajduk, D. A.; Gruner, S. M. *Macromolecules* **1996**, *29*, 1204.
(19) Huh, J.; Ikkala, O.; ten Brinke, G. *Macromolecules* **1997**, in press.
(20) Ruokolainen, J.; ten Brinke, G.; Ikkala, O.; Torkkeli, M.; Serimaa, R. *Macromolecules* **1996**, *29*, 3409.
(21) Ruokolainen, J.; Torkkeli, M.; Serimaa, R.; Komanschek, E.; Ikkala, O.; ten Brinke, G. *Phys. Rev. E* **1996**, *54*, 6646.
(22) Benoit, H.; Hadziioannou, G. *Macromolecules* **1988**, *21*, 1449.
(23) Foster, D. P.; Jasnow, D.; Balazs, A. C. *Macromolecules* **1995**, *28*, 3450.
(24) Platé, N. A.; Shibaev, V. P. *Comb-Shaped Polymers and Liquid Crystals*; Plenum Press: New York and London, 1987.
(25) Dobrynin, A. V.; Erukhimovich, I. Y. *Macromolecules* **1993**, *26*, 272.
(26) Tanaka, F. *Adv. Colloid Interface Sci.* **1996**, *63*, 23.
(27) Tanaka, F.; Ishida, M. *Macromolecules* **1997**, in press.
(28) Antonietti, M.; Conrad, J.; Thünemann, A. *Macromolecules* **1994**, *27*, 6007.
(29) Antonietti, M.; Conrad, J. *Angew. Chem., Int. Ed. Engl.* **1994**, *33*, 1869.
(30) Ikkala, O.; Ruokolainen, J.; ten Brinke, G.; Torkkeli, M.; Serimaa, R. *Macromolecules* **1995**, *28*, 7088.
(31) Ruokolainen, J.; Tanner, J.; ten Brinke, G.; Ikkala, O.; Torkkeli, M.; Serimaa, R. *Macromolecules* **1995**, *28*, 7779.
(32) Bazuin, C. G.; Tork, A. *Macromolecules* **1995**, *28*, 8877.
(33) Tal'roze, R. V.; Kuptsov, S. A.; Sycheva, T. I.; Bezborodov, V. S.; Platé, N. A. *Macromolecules* **1995**, *28*, 8689.
(34) Antonietti, M.; Burger, C.; Effing, J. *Adv. Mater.* **1995**, *7*, 751.
(35) Antonietti, M.; Maskos, M. *Makromol. Rapid Commun.* **1995**, *16*, 763.
(36) Antonietti, M.; Wenzel, A.; Thünemann, A. *Langmuir* **1996**, *12*, 2111.
(37) Ruokolainen, J.; Torkkeli, M.; Serimaa, R.; Vahvaselkä, S.; Saariaho, M.; ten Brinke, G.; Ikkala, O. *Macromolecules* **1996**, *29*, 6621.
(38) Bras, W.; Derbyshire, G. E.; Devine, A.; Clark, S. M.; Cooke, J.; Komanschek, B. E.; Ryan, A. J. *J. Appl. Crystallogr.* **1995**, *28*, 26.
(39) ten Brinke, G.; Ruokolainen, J.; Ikkala, O. *Europhys. Lett.* **1996**, *35*, 91.
(40) Ferry, J. D. *Viscoelastic properties of polymers*, 3 ed.; Wiley: New York, 1980.
(41) Doi, M.; Edwards, S. F. *The Theory of Polymer Dynamics*; Oxford University Press: New York, 1986.
(42) Fredrickson, G. H.; Larson, R. G. *J. Chem. Phys.* **1987**, *86*, 1553.
(43) Fredrickson, G. H.; Helfand, E. *J. Chem. Phys.* **1988**, *89*, 5890.
(44) Han, C. D.; Baek, D. M.; Kim, J. K. *Macromolecules* **1995**, *28*, 5886.
(45) Adams, J. L.; Graessley, W. W.; Register, R. A. *Macromolecules* **1994**, *27*, 6026.
(46) Ogawa, T.; Sakamoto, N.; Hashimoto, T.; Han, C. D.; Baek, D. M. *Macromolecules* **1996**, *29*, 2113.
(47) Ikkala, O.; Ruokolainen, J.; Torkkeli, M.; Serimaa, R.; ten Brinke, G. *Makromol. Chem., Macromol. Symp.* **1996**, *112*, 191.
(48) Stühn, B.; Mutter, R.; Albrecht, T. *Europhys. Lett.* **1992**, *18*, 427.
(49) Ehlich, D.; Takenaka, M.; Hashimoto, T. *Macromolecules* **1993**, *26*, 492.

MA961609G